Available online at www.sciencedirect.com
SCIENCE DIRECT®
Journal of Theoretical Biology 229 (2004) 101–111
Journal of Theoretical Biology
www.elsevier.com/locate/jtbi

Tamoxifen treatment failure in cancer and the nonlinear dynamics of TGFβ

Stephen Turner[a,*], Jonathan A Sherratt[a], David Cameron[b]

[a] *Centre for Theoretical Modelling in Medicine, Department of Mathematics, Heriot-Watt University, Edinburgh EH14 4AS, Scotland, UK*
[b] *Department of Clinical Oncology, Western General Hospital, Crewe Road South, Edinburgh EH4 2XU Scotland, UK*

Received 24 September 2003; received in revised form 20 February 2004; accepted 3 March 2004

Abstract

The process of cancer invasion involves a complex interplay between cell–cell and cell–medium adhesion, proteolytic enzyme secretion, cell birth and death processes, random and directed motility, and immune response, as well as many other factors. The growth factor TGFβ is known to have a complex effect on this process. It inhibits mitosis and promotes apoptosis in a concentration-dependent manner in vitro, and it is for this reason that its secretion is thought to be helpful in inhibiting tumour growth. However, recent in vitro and in vivo results have shown a significant effect of this growth factor in promoting the sensitivity of malignantly transformed cells to gradients of extracellular matrix proteins—an effect which tends to *increase* invasiveness. The drug tamoxifen has been demonstrated to be therapeutically effective in the treatment of patients with breast cancer; however, it is known also that many patients become resistant to the effect of this drug after a few years, and the reasons for this remain controversial. In this work we take our established model of cancer invasion (J. Theor. Biol. 216(1) (2002) 85), and extend it to include the effect of TGFβ. In so doing we demonstrate that a tamoxifen-stimulated upregulation of the secretion of TGFβ may give rise to a tumour which has a smaller number of cells but which has a greater invasiveness, greater metastatic potential, and a tumour histology which is known to correlate with a poorer prognosis. These data suggest that tamoxifen-stimulated secretion of TGFβ might explain treatment failure in some patients.

Keywords: Tamoxifen; Mathematical modelling; Cancer invasion; TGFβ

1. Introduction

TGFβ is secreted by both normal and malignant cells, but in the latter case expression is markedly raised. Although other growth factors are secreted by malignancies, TGFβ is of particular importance as it has a role to play in modulating the effectiveness of therapy. It has both autocrine and paracrine effects, which impact on many aspects of cell behaviour including adhesion, motility, progression through the cell cycle, secretion of enzymes and synthesis of proteins (Wakefield et al., 1991). In addition, its effects on a cell are dependent on many environmental factors such as the interaction of the cell with the extracellular matrix and the milieu of other growth factors present, as well as the state of differentiation of the cell and its position in the cell cycle. These issues may explain why it has been difficult to reproduce the in vivo behaviour in in vitro experiments, which has given rise to complex and often contradictory in vitro results (Tobin et al., 2002; Koli and Arteaga, 1996; Nakata et al., 2002). It is generally recognized that TGFβ acts as an inhibitor to cancer progression by inhibiting mitosis, and promoting apoptosis both directly and by providing chemotactic gradients recognized by immune system cells (Wiseman et al., 1988; Koli and Arteaga, 1996). However, it is also known that TGFβ can *promote* metastasis in an established malignancy by increasing the sensitivity of malignant cells to gradients of extracellular proteins by upregulating the expression of cell surface molecules associated with haptotaxis (Nakata et al., 2002). Also, TGFβ can inhibit the proliferation of cytotoxic

*Corresponding author. Institute of Petroleum Engineering, Heriot-Watt University Edinburg EH 14 4AS, UK. Tel.: +44-131-451-3609; fax: +44-13-451-3127.
E-mail addresses: stephen@ma.hw.ac.uk, stephen.turner@pet.hw.ac.uk (S. Turner).

0022-5193/$ - see front matter © 2004 Elsevier Ltd. All rights reserved.
doi:10.1016/j.jtbi.2004.03.008

lymphocytes (Koli and Arteaga, 1996), and is known also to provide a chemotactic gradient for monocytes—which in turn become activated and secrete cytokines which in turn provide chemotactic gradients for the growing tips of the endothelial cells which form the vascular bed of an established malignancy (Wiseman et al., 1988; Liss et al., 2001). Experiments in mice have shown that increased levels of peri-tumoural TGFβ correlates with increased depth of invasion, increased intraperitoneal seeding and increased lung metastasis compared with controls (see Koli and Arteaga, 1996 for a review). In addition, in vitro experiments in which a malignant cell line was cultured in the presence of TGFβ showed markedly increased motility compared with cells cultured in the absence of the growth factor. For a review of all of these findings see Arrick (1996) and Benson et al. (1996). For reviews of the biochemistry of tamoxifen, see Crommentuyn et al. (1998) and White et al. (1997).

Tamoxifen is a class of anti-cancer agents which target the oestrogen receptor, and which exercises its effects both directly through the promotion of apoptosis and the inhibition of mitosis, and indirectly through the increased expression of TGFβ. Increased levels of TGFβ both locally and systemically have been associated with tamoxifen administration in repeated studies (Chen et al., 1996; Arteaga et al., 1999). Clearly, this is a desirable effect in some respects but undesirable in others, as described above. The complex interplay between these effects may be the cause of treatment failure in some patients (Thompson et al., 1991).

In a complex nonlinear system such as this, mathematical modelling can be a useful tool in demonstrating the interplay of the various effects of the growth factor. The application of mathematics to the problem of cancer has been extensively studied through a variety of approaches. Frequently a set of coupled partial differential equations is established, in which the independent variables include tumour cell density, fibronectin and proteolytic enzyme concentration, as well as both random and directed motility. A solution of the equations is then sought either numerically (Anderson et al., 2000; Perumpanani and Norbury, 1999; Anderson and Chaplain, 1998) or analytically (Sherratt, 2000; Marchant et al., 2000,2001; Perumpanani et al., 1999). These studies have produced novel insights which have been found to be of practical use (Perumpanani et al., 1998; Gatenby and Gawlinski, 2003). However, the continuous (as opposed to discrete) approach in modelling cancer does not capture the various tumour morphologies which can be seen histologically and which are known to be closely related to metastatic potential and prognosis, and this is our particular interest here.

Our aim in this work is to use our established discrete model of cancer invasion (Turner and Sherratt, 2002) to investigate the effects of TGFβ on tumour morphology and invasiveness, and the implications which this growth hormone has for tamoxifen treatment. We concentrate in particular on ECM protein secretion, directed motility, mitosis and apoptosis. By exploring the effects on tumour progression of varying the parameters in our model we will demonstrate the circumstances under which treatment may fail, and for what reasons. In so doing we gain a better understanding of how TGFβ affects both tumour morphology and invasiveness (the two being related), and how TGFβ dynamics could best be manipulated to achieve tumour regression.

We begin by taking our established Potts model of cancer invasion (Turner and Sherratt, 2002) and explain how we have extended it to include the effects of TGFβ. We then present our studies of how tumour progression is affected by changing the parameters in the model. We show that increased synthesis of ECM proteins through the stimulation of nearby fibroblasts to produce collagen can inhibit the invasiveness of the tumour. We go on to include the effect of the growth factor on apoptosis and mitosis, and show the impact of this component of the model on tumour cell load. The dependence of the strength of the coefficient of haptotaxis on TGFβ concentration is discussed, and we show how this effect is of major importance on changing tumour morphology and invasiveness. We present some simulation results which show that, when all components of the model are taken together, there exist some regions of the parameter space in which therapy may reduce a tumour in size, but increase its depth of invasion, produce an histology which correlates with a more aggressive malignancy, and promotes greater metastatic potential. We conclude the paper by discussing the possible clinical implications of these insights.

2. The model

2.1. Outline of the Potts model

The extended Potts model has found application in particular to the problem differential adhesion driven sorting in a variety of systems (Glazier and Graner, 1993; Mombach, 1999; Stott et al., 1999; Graner and Glazier, 1992; Drasdo et al., 1995; Savill and Hogeweg, 1997). Here we give a brief overview of the model, and refer the reader to the previous work of two of the authors for greater detail (Turner and Sherratt, 2002).

The Potts model is an individual-based modelling technique which carries out simulations on a grid or lattice. We consider a discrete grid composed of individual points. In our case we take a 250×250 lattice. We attach to each point on the lattice a label σ_{ij}, and define adjacent points which have the same value of σ to lie within the same biological cell. Athough there

may be many cells present, many of them (if not all) will be of the same type. Hence, we define an additional label τ which defines the type of cell σ_{ij}. Biological cells have receptors of their surfaces associated with adhesiveness (Wijnhoven et al., 2000), and the binding of these receptors with their associated ligands either on a neighbouring cell or in the extracellular matrix gives rise to an adhesive energy. We quantify this energy by defining coupling constants J for the energy of interaction between neighbouring lattice points with differing values of σ. Hence, the total adhesive energy of the system is given by

$$E_{adh} = \sum_{ij} \sum_{i'j'} J_{\tau(\sigma_{ij})} J_{\tau(\sigma_{i'j'})}. \quad (1)$$

In addition to adhesiveness, the cells also have a potential energy associated with the elasticity of the cell membrane (Forgacs, 1998; Guck et al., 2002), and we define the elastic constant by λ. If the cells have a "relaxation volume" V_T (the volume to which they would relax in the absence of external forces), then the total energy associated with cell membrane elasticity is given by

$$E_{el} = \sum_{\sigma} \lambda (v_\sigma - V_T)^2, \quad (2)$$

where the summation runs over all of the cells in the system and v_σ is the instantaneous volume of cell σ. Bringing Eqs. (1) and (2) together we obtain the following term for the total energy of the system:

$$E_{tot} = \sum_{ij} \sum_{i'j'} J_{\tau(\sigma_{ij})} J_{\tau(\sigma_{i'j'})} + \sum_{\sigma} \lambda (v_\sigma - V_T)^2. \quad (3)$$

In evolving the simulated cellular aggregate we use the Monte Carlo method (Metropolis and Ulam, 1949). We consider copying the parameters for one lattice point (i,j) into a neighbouring lattice point (i',j'), and work out the total energy change ΔE of the system due to the copy. If this site-copy were to result in a reduction in the total energy of the system, then it is accepted. If, however, the energy would be increased then it is accepted with Boltzmann weighted probability:

$$p(\sigma_{ij} \to \sigma_{i'j'}) = \begin{cases} 1 & \text{if } \Delta E \leqslant 0, \\ e^{-\Delta E/\beta} & \text{if } \Delta E > 0, \end{cases} \quad (4)$$

where β is a parameter (analogous to temperature in other physical systems) which quantifies the likelihood of energetically unfavourable events occurring. By repeating these site-copy attempts we are able to track the evolution of the system as it attempts to reduce its total energy.

We illustrate in Fig. 1 an example of the evolution of a simulated malignant tumour under the Potts model from the authors' previous work (Turner and Sherratt, 2002).

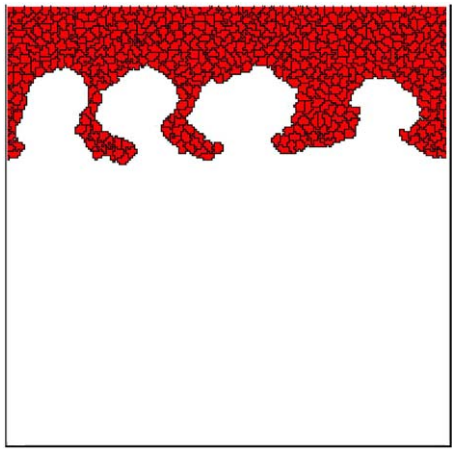

Fig. 1. Showing the characteristic appearance of a simulated tumour. From Turner and Sherratt (2002), where the simulation is described in detail. In this simulation, the cells are experiencing both cell–cell and cell–medium adhesion, and have elastic, deformable membranes. The cell mass is surrounded by extracellular matrix (ECM), and the cells secrete proteolytic enzymes which dissolve it. In so doing they create steep local gradients of ECM protein concentration which the cells are attracted to move up through the process of haptotaxis. In this manner the cells are shown to invade the ECM as long, thick strands of cells—a pattern known as "fingering", which is a hallmark of malignant invasion. Parameters used in the figure (which are described in detail in Turner and Sherratt, 2002): $J_{c-c} = 3$, $J_{c-ECM} = 6$, $k_H = 40$, $t = 1500$, $n_p = 2000$.

2.2. Secretion of TGFβ and proteolytic enzymes

Histological staining has revealed that the active forms of proteolytic enzymes are concentrated in a thin rim around the surface of the tumour (Koli and Arteaga, 1996). The explanation for this is that there exist proteins in the ECM (known as Tissue Inhibitors of MetalloProteinases—TIMPs) which act as a counterbalance to the effect of the enzymes, keeping them functional only in the region of the cells which secrete them. Similarly for TGFβ there exist ECM proteins which exercise the same inhibition. Hence, in modelling the influence of the growth factor, we assume that its effects are concentrated close to the cells which secrete it, and assume that the concentration decreases exponentially as we move away from the cell. The distance from a cell at which the concentration of the active form of the chemical has declined to negligible levels is variable, but staining suggests that it is of the order of one cell diameter (Wakefield et al., 1991). As a refinement to our earlier model, we assume also that the concentration of both proteolytic enzymes and TGFβ at a given lattice point is a linear sum of the contributions from each of the cells within a given distance from the point.

Suppose that we are considering contributions to the proteolytic enzyme concentration up to a distance d_p away, and contributions to TGFβ concentration up to

$d_{\mathscr{T}}$ away (these parameters will not, in general, be equal due to differences in the diffusion coefficients of each, and on the efficiency of neutralisation by TIMPs and their TGFβ equivalents). Then the concentration of proteolytic enzymes $\mathscr{P}_{ij}(t)$ and TGFβ, $\mathscr{T}_{ij}(t)$ will be given by

$$\mathscr{P}_{ij}(t) = k^s_{\mathscr{P}} \sum_{d=0}^{d_{\mathscr{P}}} n_{ij}(d,t) e^{-a^{\mathscr{P}} d}, \tag{5}$$

$$\mathscr{T}_{ij}(t) = k^s_{\mathscr{T}} \sum_{d=0}^{d_{\mathscr{T}}} n_{ij}(d,t) e^{-a^{\mathscr{T}} d}, \tag{6}$$

where $k^s_{\mathscr{P}}$ and $k^s_{\mathscr{T}}$ are the secretion rates of the proteolytic enzymes and TGFβ, respectively, t = time, d = distance from (i,j), $a^{\mathscr{T}}$ and $a^{\mathscr{P}}$ = rates of decay of TGFβ and proteolytic enzyme concentration respectively as one moves away from (i,j), and $n_{ij}(d,t)$ = number of cells whose closest approach to point (i,j) lies a distance d away at time t. The distances $d_{\mathscr{P}}$ and $d_{\mathscr{T}}$ are as described above. The decay rates $a^{\mathscr{T}}$ and $a^{\mathscr{P}}$ were set such that the concentrations of TGFβ and the enzymes had decayed to 0.1 at a distance $d_{\mathscr{P}}$ (or $d_{\mathscr{T}}$) away from a single cell. In our simulations we normalize the values of $\mathscr{P}_{ij}(t)$ and $\mathscr{T}_{ij}(t)$ so that they lie on a scale from 0 to 1: we do this by noting the maximum concentration of each chemical at the beginning of the simulation when the density of cell packing is at a maximum, and scale all values with respect to these maximum concentrations.

In our simulations, the influence of TGFβ on cell behaviour is determined by the mean concentration of TGFβ over the lattice points within the cell. Hence, the mean concentration of TGFβ across cell σ is given by

$$\mathscr{T}_{\sigma}(t) = \frac{1}{v_{\sigma}} \sum_{ij} \mathscr{T}_{ij}(t), \tag{7}$$

where the summation runs over all of the lattice points within cell σ, and v_{σ} is the volume of cell σ (= number of lattice points in the cell).

Now that we have expressions for the concentrations of proteolytic enzymes and TGFβ as functions of space and time, we can model the effects of each on the simulated cells.

2.3. Effects of proteolytic enzymes and TGFβ

2.3.1. Synthesis and degradation of the extracellular matrix

Proteolytic enzymes degrade the ECM, whereas TGFβ stimulates neighbouring fibroblasts to secrete it (Wakefield et al., 1991; Roberts et al., 1986). We assume that the effect of the proteolytic enzymes is to degrade the ECM in a concentration-dependent way with the change in the ECM protein density from one timestep to the next being given by

$$\Delta f^{\mathscr{P}}_{ij}(t \to t+1) = -k^f_{\mathscr{P}} \mathscr{P}_{ij}(t) f_{ij}(t), \tag{8}$$

where $f_{ij}(t)$ = ECM concentration at time t at point (i,j) and $k^f_{\mathscr{P}}$ = the efficacy with which a given concentration of the enzymes can degrade the ECM. In the case of TGFβ, we assume that the increase in the ECM protein concentration between timesteps has a linear dependence on the concentration of TGFβ at that point at the previous timestep

$$\Delta f^{\mathscr{T}}_{ij}(t \to t+1) = k^f_{\mathscr{T}} \mathscr{T}_{ij}(t), \tag{9}$$

where $k^f_{\mathscr{T}}$ quantifies the sensitivity of fibroblasts to TGFβ. This is, of course, an approximation: the rate of ECM synthesis at a given point in space will be dependent not only on the TGFβ concentration there, but also on the proximity of neighbouring fibroblasts and their sensitivity to the growth factor. This seems a reasonable approximation, however, as peri-tumoural fibroblasts are randomly distributed in space, are highly motile, and secrete ECM protein precursors for a region of space around them (Wakefield et al., 1991), all of which would give rise to a fairly even distribution of ECM. Certainly, it is the biological reality that the distribution of ECM around a tumour is fairly even (Sherratt, 2000). Taking Eqs. (8) and (9) together, we obtain the following expression for the change in $f_{ij}(t)$ during one Monte Carlo Timestep:

$$\begin{aligned} f_{ij}(t+1) &= f_{ij}(t) + \Delta f^{\mathscr{P}}_{ij} + \Delta f^{\mathscr{T}}_{ij} \\ &= [1 - k^f_{\mathscr{P}} \mathscr{P}_{ij}(t)] f_{ij}(t) + k^f_{\mathscr{T}} \mathscr{T}_{ij}(t). \end{aligned} \tag{10}$$

In Section 2.4 we explain how we have estimated the values for these parameters.

2.3.2. Mitosis

In our previous study of the Potts model applied to cancer invasion (Turner and Sherratt, 2002), we concentrated on the influence of adhesion on the probability of cell division at a given time. Using the work of (Huang and Ingber (1999)) we formed an expression for this probability which was related to the ratio between the J coupling coefficients quantifying the relative strengths of cell–cell and cell–medium adhesion. In this work, however, since we kept the values for the J coupling coefficients constant throughout, we drop this explicit dependence. Here, we need to introduce a function for the probability of division which is explicitly dependent on $\mathscr{T}_{\sigma}(t)$.

Malignant cells have a proliferation rate which is dependent on the type of carcinoma involved (Stevens and Lowe, 1995; Smith and Martin, 1973). So we assume that this is the maximum rate of cell division, and that the influence of TGFβ is to reduce it in a concentration-dependent way (Benson et al., 1996). The following functional form for the probability of mitosis

at time t as a function of TGFβ, therefore, seems reasonable

$$M_\sigma(t) = k_M\left[1 - \frac{\mathscr{T}_\sigma(t)}{\mathscr{T}_o^M + \mathscr{T}_\sigma(t)}\right], \tag{11}$$

where k_M = maximum proliferation rate (corresponding to the proliferation rate in the absence of TGFβ) and $\mathscr{T}_o^M$ is a constant which controls sensitivity of the cell to increases in $\mathscr{T}_\sigma$. The form of this function is illustrated in Fig. 5. When a cell is selected to undergo mitosis, it is divided through its centre along the axis of minimum diameter, as observed in vitro (Mombach et al., 1993).

2.3.3. Apoptosis

The tendency of TGFβ is to promote apoptosis occurs in a variety of ways. It can happen directly through binding to cell surface molecules and triggerring cell death through intracellular signalling (Perry et al., 1995). Or it may occur indirectly through a variety of mechanisms: for example, through providing chemotactic gradients which are recognised by cytotoxic cells of the immune system (Arrick, 1996), promoting the growth of capillaries which increase therapeutic access, and increasing the local density of ECM protein—which can inhibit directed motility. We assume that this increasing probability of apoptosis can be modelled using a function of the form

$$A_\sigma(t) = \frac{k_A\mathscr{T}_\sigma}{\mathscr{T}_o^A + \mathscr{T}_\sigma(t)}, \tag{12}$$

which allows us to vary both the maximum rate of apoptosis (through k_A) and the sensitivity of both the malignant cells as well as the cells of the immune system to TGFβ (through $\mathscr{T}_o^A$). The form of this function is shown in Fig. 5. When a cell is selected to be killed through apoptosis, all of the lattice points which it contains are changed from σ_{ij} to zero.

2.3.4. Directed motility

It is known from in vivo experiments in mice that the increased expression of TGFβ is associated with an increase in intra-peritoneal invasion, increased secondary deposits in the lungs and increased serum TGFβ levels (Koli and Arteaga, 1996). Also, it is known from both in vivo and in vitro experiments that TGFβ has a tendency to increase the sensitivity of malignant cells to ECM protein gradients through the upregulation of genes which code for cell surface molecules associated with directed motility (Nakata et al., 2002)—a process which takes around 24 h. Since one MCS in our simulation corresponds in real time to a few minutes, it seems appropriate to consider not the instantaneous values of $\mathscr{T}_\sigma$, but instead the mean value taken over all of the cells. In Fig. 2 we illustrate the distribution of values of TGFβ for a typical simulation: as we can see, the distribution has a range of values determined by the choice of $k_{\mathscr{T}}^s$. In considering the influence of TGFβ on a process which takes place on a timescale of around 24 h, therefore, it seems appropriate to use the mean value of the distribution. We propose that the relationship between the coefficient of haptotaxis and TGFβ will be related to the mean cell TGFβ concentration through

$$k_H \propto \sum_{\sigma=1}^{N} \mathscr{T}_\sigma, \tag{13}$$

where T_σ is the mean TGFβ concentration over cell σ, and the summation runs over all of the cells. This estimate of the relationship is, of course, an approximation—one study suggests that the relationship may be steeper than this (Nakata et al., 2002). However, we make this simplest estimate as a first approximation. This coefficient increases the likelihood of site-swap events occurring in the direction of increasing fibronectin concentration, by adding a factor $k_H(f_{ij} - f_{i'j'})$ to ΔE in Eq. (4). If the site-swap attempt occurs in the

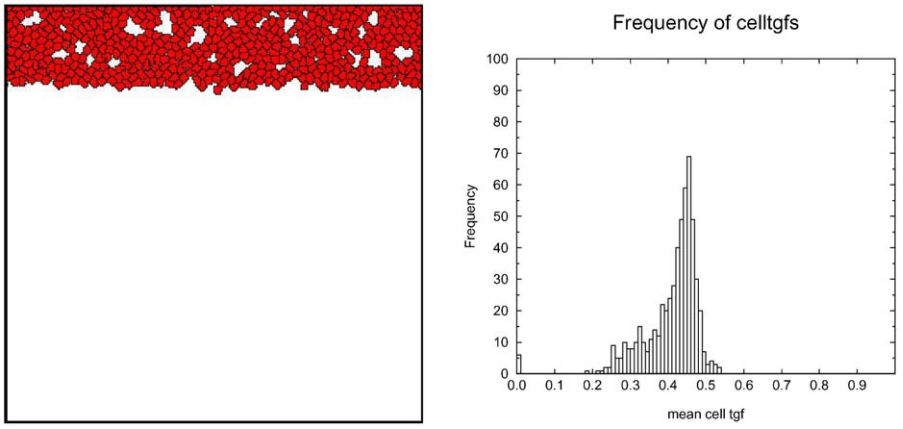

Fig. 2. An image from the simulation along with a histogram showing its distribution of values of T_σ ($t = 200$ MCS, $k_{\mathscr{T}}^s = 0.5$, $k_{\mathscr{P}}^s = 1.0$, $d_{\mathscr{T}} = d_{\mathscr{P}} = 6$, $J_{cc} = J_{cm} = 6$, $\lambda = 1$, $\beta = 8$).

direction of increasing fibronectin concentration, then there is an increased probability of it being accepted.

2.4. Results

2.4.1. Parameter values

All of the simulations were conducted on a 250×250 grid, with the following Potts parameters remaining the same throughout: $J_{cc} = 6$, $J_{cm} = 6$, $\lambda = 1$, $\beta = 8$, $V_T = 25$. In Section 2 we introduced several new parameters quantifying the secretion rates of TGFβ and the proteolytic enzymes, as well as the tendency of TGFβ to increase ECM protein secretion, promote apoptosis and inhibit mitosis. Considering first the secretion rates, the normalization procedure which we described earlier ensures that the concentrations $\mathscr{T}_{ij}(t)$ and $\mathscr{P}_{ij}(t)$ lie between 0 and 1, so the secretion rates $k^s_{\mathscr{T}}$ and $k^s_{\mathscr{P}}$ can be defined also to lie on this scale, with 0 corresponding to no secretion and 1 to maximal secretion. In making estimates of the parameters $k^f_{\mathscr{T}}$ and $k^f_{\mathscr{P}}$ we chose a value for the rate of decay of the ECM which ensured that the ECM protein concentration of a lattice point continually occupied by a cell had been significantly reduced after 1000 MCS. One Monte Carlo timestep corresponds to a few minutes in real time. Hence, 1000 MCS corresponds to over 24 h: in vitro studies of the rate at which proteolytic enzymes can dissolve the matrix support the assumption that the ECM protein concentration will have been significantly reduced on this timescale (Perumpanani and Byrne, 1999). We chose values for $k^f_{\mathscr{P}}$ which keep this rate of dissolution approximately the same. In the case of $k^f_{\mathscr{T}}$, obviously the rate of synthesis of ECM in the case of an invading malignancy will be less than the rate of dissolution by enzymes, otherwise invasion could not progress (of course, there is the case where excessive ECM synthesis gives rise to a fibrous capsule around the tumour, but this case only needs to be considered if we are dealing with benign or low-grade tumours, and is not relevant to our consideration of an aggressive, invasive malignancy). We assume that the rate of synthesis of ECM protein due to TGFβ stimulus acts on a similar timescale to the dissolution of ECM by proteolytic enzymes (as described above), and set the value of $k^f_{\mathscr{T}}$ accordingly.

In the case of parameter values for the mitosis and apoptosis probability functions (11) and (12), we note from the studies of Smith and Martin (1973) that in the case of an aggressive rat sarcoma, the majority of cells had undergone one cell division within 20 h. In our simulation, we set the maximum probability of mitosis—corresponding to k_M in Eq. (11)—to 0.02. This ensured that all cells had a high probability of undergoing at least one division within <1000 MCS. We set the probability of apoptosis to lie on a similar scale, as it is known from both clinical and laboratory studies that the level of apoptosis in clinical tumours parallels that of proliferation (Cameron et al., 1997,2001). In addition, the term which we have used to model apoptosis can be modulated to take into account the promotion of apoptosis by a robust immune response complimented by medical intervention.

2.4.2. ECM protein concentration, directed motility, and invasiveness

In Fig. 3 we illustrate two cases: first, the evolution of the tumour when TGFβ secretion is not included (left), and, second, where it has been included (right). In both cases the proteolytic enzymes are doing their work of dissolving the ECM, and the coefficient of haptotaxis is high. As we can see, the tumour initially has a ragged appearance and releases showers of cells, both individually and in small islands—a hallmark of an aggressive malignancy (Stevens and Lowe, 1995). However, the introduction of the secretion of TGFβ (with its capacity

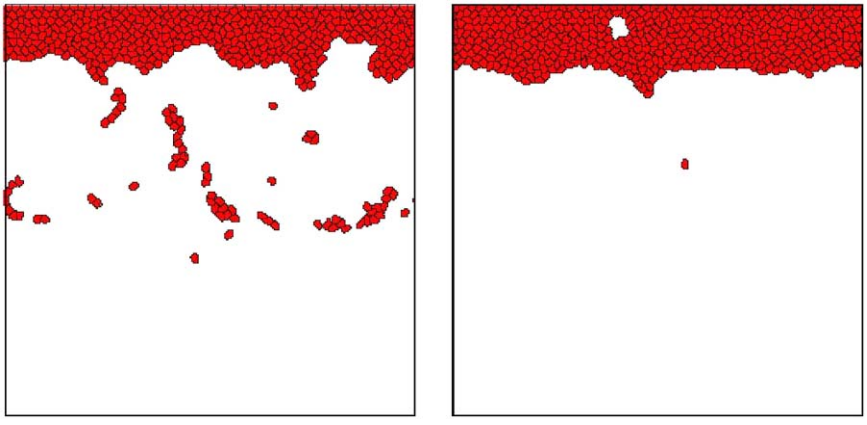

Fig. 3. Illustrating the morphology and invasiveness of the invading front in the presence of proteolytic enzyme secretion, but with TGFβ secretion absent (left), and included (right). In the presence of TGFβ secretion the invasiveness has been markedly reduced, and the tumour surface is far smoother. This would correspond histologically to a less aggressive malignancy. (In both figures: $k_H = 40$, $k^s_{\mathscr{T}} = 0$, $k^s_p = 0.5$, $k^f_p = 0.02$, $d_{\mathscr{T}} = 2$, $d_{\mathscr{P}} = 2$, $J_{cc} = J_{cm} = 6$, $\lambda = 1$, $\beta = 8$; with TGFβ secretion included, in addition: $k^s_{\mathscr{T}} = 0.5$, $k^f_{\mathscr{T}} = 0.015$.)

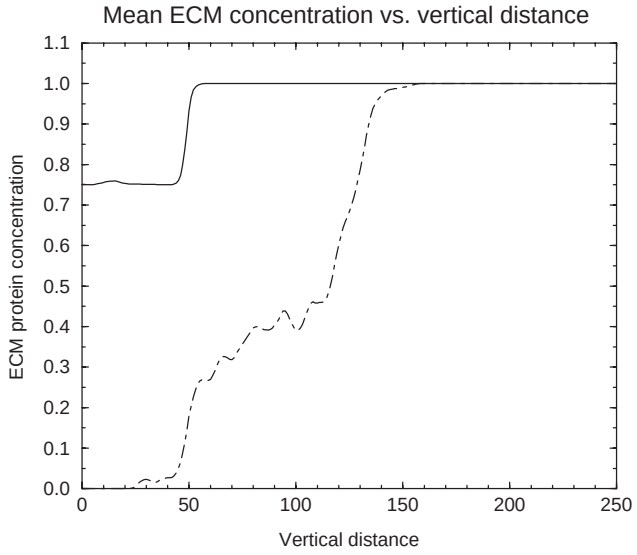

Fig. 4. The variation in the mean ECM protein concentration taken at horizontal cross-sections through the simulations illustrated in Fig. 3 with vertical distance. As we can see, in the absence of TGFβ secretion (dashed curve) there is a steep haptotactic gradient which gives rise to deep invasiveness and an infiltrative pattern of invasion. Conversely, when TGFβ secretion is increased (solid curve), the synthesis of new ECM gives rise to a shallower gradient, markedly reduced invasion, and a diffuse pattern of invasion. Parameters for each of the curves are given in the caption to Fig. 3.

to slow the decrease in the ECM protein concentration through the stimulation of peri-tumoural fibroblasts) causes the invasiveness of the tumour to be greatly reduced. In this case, although there do exist a few isolated cells invading the ECM, they are much reduced in number. We can understand the mechanisms for this better through an inspection of Fig. 4, which shows the variation in the mean ECM protein concentration taken at horizontal cross-sections as we move vertically down the screen shots. In the case where $k^s_{\mathcal{T}} = 0$ (i.e. no TGFβ secretion) there is a steep haptotactic gradient which promotes strong invasion. Conversely, when we increase the secretion rate of TGFβ the gradient is made more shallow, and invasiveness is reduced.

2.4.3. Mitosis and apoptosis

In Fig. 5 we show the probability functions for mitosis and apoptosis superimposed on a histogram for the distribution of $\mathcal{T}_\sigma$ for the set of parameters listed in the caption, along with an image illustrating the corresponding tumour when the coefficient of haptotaxis is set to zero. The majority of the cells have a value of TGFβ at which it is more likely for cells to die through apoptosis than to proliferate. We would expect, therefore, that the cell mass would progressively reduce in size at this rate of TGFβ secretion, and the associated image illustrates that this is the case. Clinically, this would correspond to remission of the tumour, assuming that high levels of TGFβ secretion were to be maintained.

In Fig. 6 we see the converse situation (with haptotaxis still set to zero): here the TGFβ secretion rate is reduced, and the cells have a higher probability of proliferation compared with apoptosis. The associated image shows that there is a progressive increase in tumour load. Notice also that in this case there is less cell-free space within the cells mass compared with Fig. 5, due to the cells rapidly multiplying when they have fewer cells around them—and, consequently, have a lower mean cell TGFβ concentration. This decreased free space corresponds to an increase in cell density within the cell mass. Once again in this simulation we have set the coefficient of haptotaxis to zero. Notice, however, that even though there is no directed motility, the cell mass nevertheless has a less ragged appearance when the number of cells present is increased. Histologically, tumours which have a ragged morphology tend to invade more aggressively compared with a tumour which has a smoother surface, even though they may be smaller. The implications of this are discussed more extensively in Section 3.

We conclude from these two simulations, therefore, that increasing the TGFβ secretion rate can reduce the tumour load, but assists in the creation of a tumour morphology which is know to correlate with greater potential for invasion and metastasis, even in the absence of directed motility.

2.4.4. The net effect of TGFβ dynamics on tumour morphology

We have studied the effect of ECM synthesis and degradation, proliferation, and apoptosis separately in order to gain a better understanding of how each of these factors influence the model. Now we bring all of these components together to study their combined effects on the evolution of the simulated tumour.

In Fig. 7 we have taken the simulations corresponding to Figs. 5 and 6, and have added directed motility. The effect of this is to "pull" the cells at the tip of the invading front further into the ECM and away from their neighbours. This causes their local TGFβ concentration to drop, which causes them to have an increased probability of mitosis (this corresponds to a movement of the cell to the left of the histogram distributions illustrated in Figs. 5 and 6). Hence, when a cell has empty space around it, the resulting increased probability of mitosis makes it likely that the space will be filled by daughter cells. This explains the increased cell number and increased depth of invasion in Fig. 7 where TGFβ secretion is low (the leftmost image).

In Fig. 7 (right image) we have taken the simulation corresponding to Fig. 6 and added strong directed motility at a level $k_H = 70$. The effect of this is to produce a marked increase in the invasiveness of the

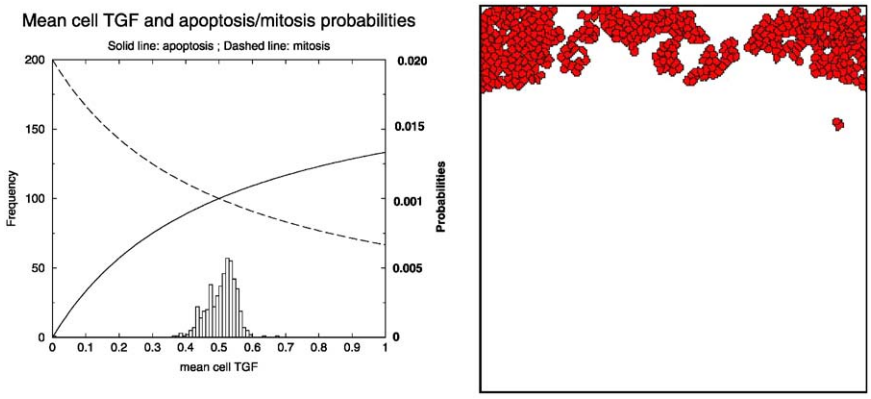

Fig. 5. The probability functions for apoptosis and mitosis superimposed on a histogram of the $\mathscr{T}_\sigma$ distribution for the case where TGFβ secretion is high and haptotaxis is set to zero, along with an image of the simulated tumour under these conditions. The coefficient of haptotaxis has been set to zero so that we can investigate the effects of apoptosis and mitosis alone on the evolution of the tumour. Most cells have a value of $\mathscr{T}_\sigma$ which results in a higher probability of apoptosis compared with mitosis. Cells which have many neighbours nearby will tend to lie in the histogram bins to the right of the distribution, and, hence, will have an increased probability of apoptosis compared with those which are isolated. The effect of this is for dense clusters of cells to be less likely, and for the creation of small groups surrounded by empty space to be more likely. This is the case, as we can see from the image. Histologically, this appearance would correspond to a "infiltrative" pattern of invasion, with isolated showers of cells moving into the surrounding healthy tissue and resulting in a high probability of early metastasis ($k^s_{\mathscr{T}} = 0.7$, $k^s_{\mathscr{P}} = 1.0$, $k^f_{\mathscr{P}} = 0.02$, $k^s_{\mathscr{T}} = 0.005$, $k_H = 0$, $d_{\mathscr{T}} = d_{\mathscr{P}} = 2$, $k_M = k_A = 0.02$, $\mathscr{T}^M_o = \mathscr{T}^A_o = 0.5$, $d_{\mathscr{T}} = 2$, $d_{\mathscr{P}} = 2$).

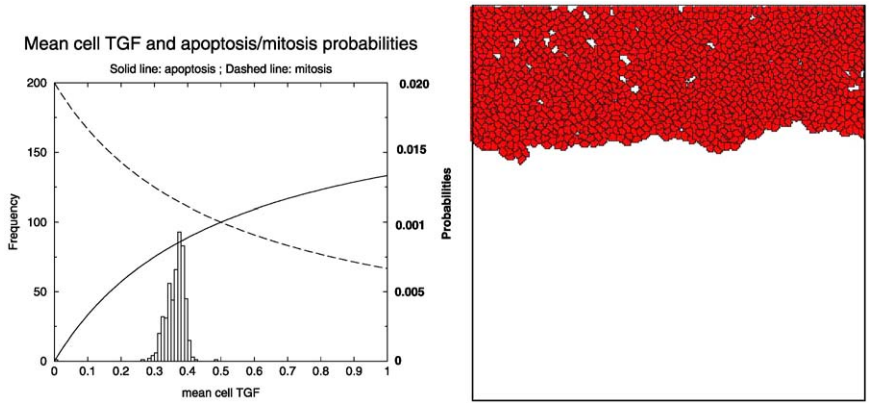

Fig. 6. The probability functions for apoptosis and mitosis superimposed on a histogram of the $\mathscr{T}_\sigma$ distribution for the case where TGFβ secretion is low and haptotaxis is set to zero, along with an image of the simulated tumour under these conditions. This image should be compared with that in Fig. 5. In this case, mitosis is more probable than apoptosis across the range of $\mathscr{T}_\sigma$. Cells which have few neighbours have a lower mean $\mathscr{T}_\sigma$, and, hence, an increased probability of mitosis; hence, isolated cells tend to multiply quickly, filling the space around them. This explains the increased density of cells in the image, and a reduction in the fragmentation seen in Fig. 5. Histologically, this corresponds to a "diffuse" pattern of invasion, which tends to move more slowly into healthy tissue and corresponds to a less aggressive tumour ($k^s_{\mathscr{T}} = 0.5$, $k^s_{\mathscr{P}} = 1.0$, $k^f_{\mathscr{P}} = 0.02$, $k^s_{\mathscr{T}} = 0.005$, $k_H = 0$, $d_{\mathscr{T}} = d_{\mathscr{P}} = 2$, $k_M = k_A = 0.02$, $\mathscr{T}^M_o = \mathscr{T}^A_o = 0.5$).

tumour and a very fragmented, infiltrative pattern of invasion. This situation would correspond histologically to a high-grade malignancy with strong metastatic potential. It is interesting to compare the two images and notice that in the leftmost figure, although there are a greater number of cells present, the tumour presents a less invasive morphology. Our conclusion from these results, therefore, is that in the scenario where directed motility is strongly enhanced by TGFβ secretion, it is possible to promote the development of a tumour which is smaller in size but which represents a far greater metastatic risk.

3. Discussion and therapeutic implications

Our simulations have allowed us to draw several important conclusions regarding the behaviour of a tumour responding to TGFβ secreted by its cells. To summarize:

- TGFβ reduces the rate of dissolution of ECM proteins, giving rise to a shallower haptotactic gradient. In the absence of any changes to the coefficient of haptotaxis, this has the effect of inhibiting the tumour's invasiveness. However, this

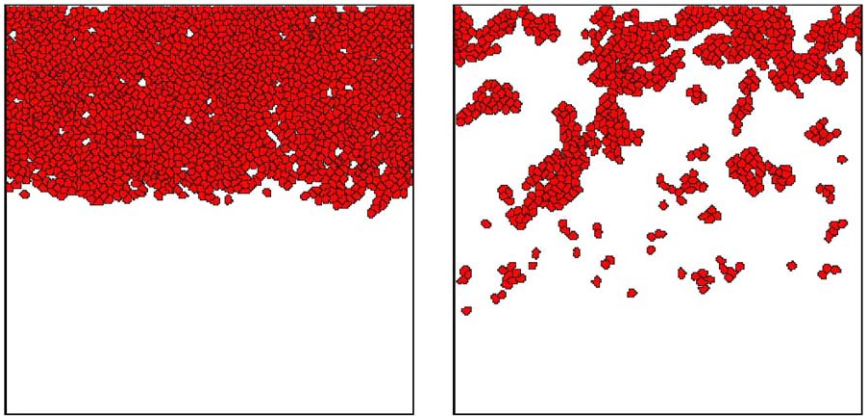

Fig. 7. Left: the evolution of the tumour under the situation illustrated in Fig. 6, but in this case with directed motility included at a low level. Right: the evolution of Fig. 5 with directed motility included. The effect of including motility in the case for low TGFβ secretion (left) is to pull individual cells away from their neighbours and, through the mechanism described in the caption to Fig. 6, promote cell division and produce a diffuse pattern of invasion. Conversely, in the case for high TGFβ secretion (right), including directed motility has the effect of pulling isolated cells away from the main tumour mass, which then invade alone or in small islands. This corresponds to a "infiltrative" pattern of invasion, which is the hallmark of an aggressive malignancy ($k_H = 20$, $k^s_{\mathcal{F}} = 0.7$, $k^s_p = 0.5$, $k^f_p = 0.02$, $k^f_{\mathcal{F}} = 0.015$, $d_{\mathcal{F}} = 2$, $d_{\mathcal{P}} = 2$).

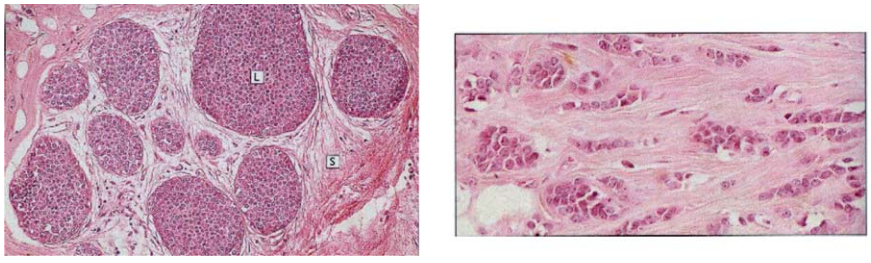

Fig. 8. Photomicrographs showing a lobular carcinoma in situ of the breast (left) and an invasive lobular carcinoma (right). In the figure on the left there are lobules (L) which are increased in size and packed with atypical cells. The basement membrane remains intact and there is no invasion of the stroma (S). However, in the figure on the right we see invasion in the form of narrow cords of cells—a phenomenon known as "Indian file" invasion (Stevens and Lowe, 1995).

inhibition can be overcome if the sensitivity of cells to a haptotactic gradient is increased. The ranges of action of both the proteolytic enzymes and TGFβ around the invading front also have a role to play in determining the invasiveness.

- TGFβ has a tendency to inhibit mitosis and promote apoptosis, giving rise to a smaller tumour. However, if the effect on directed motility is to significantly increase the coefficient of haptotaxis then a smaller but more aggressive malignancy can be the result.

The utility of the extended Potts model in simulating tumour growth is that it produces solutions which bear a close resemblance to actual tumour histologies. Consider Fig. 8 which shows photomicrographs of a lobular carcinoma in situ and an invasive lobular carcinoma, and note that the former is known clinically to turn into the latter in about a third of cases (Stevens and Lowe, 1995).

Through our study we have been able to show how histologies such as that shown in Fig. 8 can develop. If we compare the invasive picture with our simulation study in Fig. 7 with TGFβ included at a high level (the right image) we see that there are similarities: invasion is taking place in the form of individual cells or islands of cells, some of which have an elongated appearance. Fig. 7 was generated through including an increase in the coefficient of haptotaxis due to increased secretion of TGFβ as well as a concentration-dependent modulation of mitosis and apoptosis. "Indian file" invasion is a form of malignant invasion which has the appearance illustrated in Fig. 8 with strings of invading cells forming narrow columns. It is a hallmark of an aggressively invading malignancy. If we compare the histological appearance of the invading cells in Fig. 8 with the simulation in Fig. 7 (right image) we can see a similarity in that both the simulated and real cells are invading in the form of small islands and strings. Given these similarities we propose that TGFβ may have a role to play in determining the macroscopic morphology of some types of tumour, and that "Indian file" invasion in particular may be promoted by TGFβ induced increases

in directed motility. In order to test this hypothesis it would be necessary to determine several characteristics of TGFβ secreting malignant cells. In particular, it would be useful to take cells from tumours known to have a characteristic appearance and investigate their dependence on increasing concentrations of TGFβ in vitro. To the best of our knowledge, although assays of directed motility have elucidated a link between TGFβ and increases in haptotaxis (Nakata et al., 2002), correlating these findings with particular types of carcinoma or particular tumour morphologies has not been done. This would be an interesting experimental study, which would help to illuminate the relationship between the microscopic behaviour of malignant cells and the macroscopic morphology of the tumours which they form.

These results may also give us some insights into the efficacy of tamoxifen therapy, and possibly causes for its failure in some patients. It is well-known that patients being treated with this drug frequently respond well to begin with, but become resistant to its effects after a period of some years. Attempts to explain this have concentrated on mutations to the oestrogen receptor as the most likely cause (Tonetti and Jordan, 1997). However, the evidence for this being the cause is controversial, and it is possible that treatment failure is due to changes in TGFβ responsiveness and secretion (Thompson et al., 1991). Our study models secondary resistance, which is almost certainly not due to mutations, but perhaps adaptation of the cell to grow due to increased drive from the TGFβ pathway. We suggest that the TGFβ-induced impact on mitosis, apoptosis and directed motility is implicated in treatment failure. The effect of tamoxifen is directly to induce apoptosis in malignant cells, and to promote the secretion of TGFβ and achieve tumour regression as a consequence (Chen et al., 1996; Perry et al., 1995). However, if a patient is suffering from a malignancy composed of a cell type which is highly sensitive to changes in directed motility following increases in TGFβ secretion, our results suggest that tamoxifen therapy may give rise to a tumour which is smaller but which has a higher capacity for invasion due to changes in the morphology of the invading front. It may be possible to test this hypothesis in vivo using an animal model, by seeding malignant cell lines known from in vitro studies to have a coefficient of haptotaxis which is sensitive to increases in TGFβ concentration. One could then treat some of the animals with tamoxifen and investigate the effect on tumour morphology compared with untreated controls. If it was discovered that an infiltrative morphology was induced by tamoxifen, then it would be worth considering whether tamoxifen should be given to such patients, or whether it should be supplemented by other drugs to increase the probability of apoptosis.

A question which we have not addressed is the phenomenon of tamoxifen treatment withdrawal promoting or inhibiting the growth of residual tumour. Many women complain that their breast cancer relapses not long after stopping tamoxifen, which is now routinely given for 5 years. In addition, there exists laboratory data that long-term tamoxifen therapy in xenografts can cause tumours to become dependent on tamoxifen for growth. Simulating the situation where tamoxifen withdrawal may give a growth stimulus to the residual tumour which has become (as shown by our model) more invasive would be an obvious extension to this work.

To conclude, our study has shown a link between directed motility and macroscopic tumour morphology in our simulations. This link could have an impact on our approach to the therapeutic inhibition of cancer invasion if it is shown to be a real effect in vivo, and we have proposed experiments to help determine whether this is the case.

References

Anderson, A.R.A., Chaplain, M.A.J., 1998. Continuous and discrete mathematical models of tumor-induced angiogenesis. Bull. Math. Biol. 60, 857–899.

Anderson, A.R.A., Chaplain, M.A., Newman, E.L., Steele, R.J.C., Thompson, A.M., 2000. Mathematical modelling of tumour invasion and metastasis. J. Theor. Med. 2, 129–154.

Arrick, B.A., 1996. Therapeutic implications of the TGF-β system. J. Mamm. Gland Biol. Neoplasia 1 (4), 391–397.

Arteaga, C.L., Koli, K.M., Dugger, T.C., Clarke, R., 1999. Reversal of tamoxifen resistance of human breast carcinomas in vivo by neutralising antibodies to transforming growth factor-β. J. Natl. Cancer Inst. 91 (1), 46–53.

Benson, J.R., Baum, M., Colletta, A.A., 1996. Role of TGFβ in the anti-estrogen response/resistance of human breast cancer. J. Mamm. Gland Biol. Neoplasia 1 (4), 381–389.

Cameron, D.A., Ritchie, A.A., Langdon, S., Anderson, T.J., Miller, W.R., 1997. Tamoxifen induced apoptosis in zr-75 breast cancer xenografts antedates tumour regression. Breast Cancer Res. Treat. 45 (2), 99–107.

Cameron, D.A., Ritchie, A.A., Miller, W.A., 2001. The relative importance of proliferation and cell death in breast cancer growth and response to tamoxifen. Eur. J. Cancer 37 (12), 1545–1553.

Chen, H., Tritton, T.R., Kenny, N., Absher, M., Chiu, J.F., 1996. Tamoxifen induces TGF-β1 activity and apoptosis of human MCF-7 breast cancer cells in vitro. J. Cell. Biochem. 61, 9–17.

Crommentuyn, K.M., Schellens, J.H., van den Berg, J.D., Beijnen, J.H., 1998. In-vitro metabolism of anti-cancer drugs, methods and applications: paclitaxel, docetaxel, tamoxifen and ifosfamide. Cancer Treat. Rev. 24 (5), 345–366.

Drasdo, D., Kree, R., McCaskill, J.S., 1995. Monte carlo approach to tissue-cell populations. Phys. Rev. E 52 (6B), 6635–6657.

Forgacs, G., 1998. Surface tension and viscoelastic properties of enbryonic tissues depend on the cytoskeleton. Biol. Bull. 194, 328–330.

Gatenby, R.A., Gawlinski, E.T., 2003. The glycolytic phenotype in carcinogenesis and tumor invasion: insights through mathematical models. Cancer Res. 63 (14), 3847–3854.

Glazier, J.A., Graner, F., 1993. Simulation of the differential adhesion driven rearrangement of biological cells. Phys. Rev. E 47 (3), 2128–2154.

Graner, F., Glazier, J.A., 1992. Simulation of biological cell sorting using a two-dimensional extended potts model. Phys. Rev. Lett. 69 (13), 2013–2016.

Guck, J., Ananthakrishnan, R., Cunningham, C.C., Kas, J., 2002. Stretching biological cells with light. J. Phys.—Cond. Matter 14 (19), 4843–4856.

Huang, S., Ingber, D.E., 1999. The structural and mechanical complexity of cell-growth control. Nat. Cell Biol. 1, E131–E138.

Koli, K.M., Arteaga, C.L., 1996. Complex role of tumor cell transforming growth factor (TGF)-βs on breast carcinoma progression. J. Mamm. Gland Biol. Neoplasia 1 (4), 373–380.

Liss, C., Fekete, M.J., Hasina, R., Lam, C., Lingen, M.W., 2001. Paracrine angiogenic loop between head and neck squamous cell carcinomas and macrophages. Int. J. Cancer 93 (6), 781–785.

Marchant, B.P., Norbury, J., Perumpanani, A.J., 2000. Traveling shock waves arising in a model of malignant invasion. SIAM J. Appl. Math. 60 (2), 463–476.

Marchant, B.P., Norbury, J., Sherratt, J.A., 2001. Travelling wave solution to a haptotaxis dominated model of malignant invasion. Nonlinearity 14, 1653–1671.

Metropolis, N., Ulam, S., 1949. The Monte Carlo method. J. Am. Stat. Soc. 44 (247), 335–341.

Mombach, J.C.M., 1999. Simulation of embryonic cell self-organization: a study of aggregates with different concentrations of cell types. Phys. Rev. E 59 (4), R3827–R3830.

Mombach, J.C.M., Rita, M.C. de Almieda, Iglesias, J.R., 1993. Mitosis and growth in biological tissues. Phys. Rev. E 48 (1), 598–602.

Nakata, D., Hamada, J., Ba, Y., Matsushita, K., Shibata, T., Hosokawa, M., Moriuchi, T., 2002. Enhancement of tumorigenic, metastatic and in vitro invasive capacity of rat mammary tumor cells by transforming growth factor-β. Cancer Lett. 175, 95–106.

Perry, R.R., Kang, Y., Greaves, B.R., 1995. Relationship between tamoxifen-induced transforming growth factor β expression, cytostasis and apoptosis in human breast cancer cells. Br. J. Cancer 72, 1441–1446.

Perumpanani, A.J., Byrne, H.M., 1999. Extracellular matrix concentration exerts selection pressure on invasive cells. Eur. J. Cancer 35 (8), 1274–1280.

Perumpanani, A.J., Norbury, J., 1999. Numerical interactions of random and directed motility during cancer invasion. Math. Comp. Model. 30, 123–133.

Perumpanani, A.J., Simmons, D.L., Gearing, A.J.H., Miller, K.M., Ward, G., Norbury, J., Schneemann, M., Sherratt, J.A., 1998. Extracellular matrix-mediated chemotaxis can impede cell migration. Proc. R. Soc. London B 265, 2347–2352.

Perumpanani, A.J., Sherratt, J.A., Norbury, J., Byrne, H.M., 1999. A two-parameter family of travelling waves with a singular barrier arising from the modelling of extracellular matrix mediated tumour invasion. Physica D 126, 145–159.

Roberts, A.B., et al., 1986. Transforming growth factor type β: rapid induction of fibrosis and angiogenesis in vivo and stimulation of collagen formation in vitro. Proc. Natl. Acad. Sci. 83, 4167–4171.

Savill, N.J., Hogeweg, P., 1997. Modelling morphogenesis: from single cells to crawling slugs. J. Theor. Biol. 184, 229–235.

Sherratt, J.A., 2000. Traveling wave solutions of a mathematical model for tumor encapsulation. SIAM J. Appl. Math 60 (2), 392–407.

Smith, J.A., Martin, L., 1973. Do cells cycle? Proc. Natl. Acad. Sci. 70 (4), 1263–1267.

Stevens, A., Lowe, J., 1995. Pathology. Mosby, St. Louis, MO.

Stott, E.L., Britton, N.F., Glazier, J.A., Zajaz, M., 1999. Stochastic simulation of benign avascular tumour growth using the Potts model. Math. Comp. Model. 30, 183–198.

Thompson, A.M., Kerr, D.J., Steel, C.M., 1991. TGFβ1 is implicated in the failure of tamoxifen therapy in human breast cancer. Br. J. Cancer 63, 609–614.

Tobin, S.W., Dourville, K., Banbow, U., Brinckerhoff, C.E., Memoli, V.A., Arrick, B.A., 2002. Consequences of altered TGFβ expression and responsiveness in breast cancer: evidence for autocrine and paracrine effects. Oncogene 108–118.

Tonetti, D.A., Jordan, V.C., 1997. The role of estrogen receptor mutations in tamoxifen-stimulated breast cancer. J. Steroid Biochem. Mol. Biol. 62 (2/3), 119–128.

Turner, S., Sherratt, J.A., 2002. Intercellular adhesion and cancer invasion: a discrete simulation using the extended Potts model. J. Theor. Biol. 216 (1), 85–100.

Wakefield, L.M., Colletta, A.A., McCune, B.K., Sporn, M.E., 1991. Roles for transforming growth factor β's in the genesis, prevention and treatment of breast cancer. In: Dickson, R.B., Lippman, M.E. (Eds.), Genes, Oncogenes and Hormones: Advances in Cellular and Molecular Biology of Breast Cancer. Kluwer Academic Publishers, Boston, pp. 97–136.

White, I.N., Martin, E.A., Styles, J., Lim, C.K., Carthew, P., Smith, L.L., 1997. The metabolism and genotoxicity of tamoxifen. Prog. Clin. Biol. Res. 396, 257–270.

Wijnhoven, B.P.L., Dinjens, W.N.M., Pignatelli, M., 2000. E-cadherin–catenin cell–cell adhesion complex and human cancer (review). Br. J. Surgery 87, 992–1005.

Wiseman, D.M., Polverini, P.J., Kamp, S.J., Leibovich, D.W., 1988. TFGβ1 is chemotactic for human monocytes and induced their expression of angiogenic activity. Biochem. Biophys. Res. Comm. 793–800.